Wide-Scanning-Angle Leaky-Wave Array Antenna Based on Microstrip SSPPs-TL

Dujuan Wei, Jianying Li, *Member, IEEE*, Jiangjun Yang, Yiangxiao Qi, and Guangwei Yang

***Abstract*—In this letter, a wide-scanning-angle leaky-wave antenna (LWA) based on a microstrip spoof surface plasmon polaritons (SSPPs) transmission line (TL) is proposed. The dual-conductor SSPPs-TL as the guiding-wave structure of the proposed antenna consists of a two-edged grooved corrugated strip and a ground plane. A set of metallic posts connect the corrugated strip to the ground plane along two sides of the SSPPs-TL in a staggered way, which converts SSPPs to radiation waves. A power divider is the feeding network for two antenna arrays. The scanning region is mainly controlled by the depth of the groove, which has strong relationship with the dispersion of the antenna. Over the operating band from 5 to 7 GHz, the beam of the proposed antenna scans widely from −30° to 51° (including the broadside) with the realized gain varying from 15.9 to 19.4 dBi. A prototype is fabricated and measured, which confirms the design theory and the simulation results.**

***Index Terms*—Leaky-wave antenna (LWA), spoof surface plasmon polaritons (SSPPs), microstrip SSPPs-transmission line (TL), wide scanning angle.**

I. Introduction

DUE to the outstanding merits of simple feeding network, high directivity, and frequency-scanning property, leaky-wave antennas (LWAs) have attracted much attention recently for their applications in radar systems, wireless communication systems, and surveillance systems [1].

Surface plasmon polaritons (SPPs) represent a surface wave that can be tightly confined within the interface of two materials with two opposite permittivities [2]. In the optical region, the SPPs can be tightly confined in the interface of the metal and dielectrics. However, the natural SPPs cannot be supported and propagated in the microwave- and terahertz-frequency band because the metal behaves as a perfect electric conductor (PEC), which does not have negative permittivity. In microwave and terahertz frequency, spoof SPPs (SSPPs) are introduced to mimic the SSPs-like performances in the optical region, such as the dispersion relation and high spatial confinement [3], [4]. The plasmonic metamaterials supporting SSPPs are usually generated by periodical subwavelength holes, grooves, and slits. However, these plasmonic metamaterials have major limitations in engineering applications because of three-dimensional geometries. Therefore, an ultrathin SSPPs waveguide, formed from a corrugated metal strip with single or dual grooves, was proposed recently [5], [6].

Several LWAs based on the ultrathin SSPPs waveguide were reported recently [7]–[9]. A broad-angle beam-scanning LWA fed by the ultrathin SSPPs waveguide is proposed in [7]. Six circular patches are placed near the single-layer SSPPs waveguide, which has dual main beams scanning from −30° to 25°. Two ways of converting SSPPs to radiation waves are described in [8] by periodically modulating the SSPPs waveguide in either a symmetrical or an asymmetrical manner. For the symmetrical modulated antenna, the radiation patterns are omnidirectional in E-plane and the beams scan in the elevation plane. For the asymmetrical antenna, the main beam is single but scans in the azimuth plane. Both the scanning regions are narrow with approximately 20°. Kianinejad *et al.* [9] propose a single-layered meander SSPP cell LWA, which can generate the radiating space harmonics. The antenna is able to cover the wide scanning region against the frequency, but the two main beams in the upper and lower free spaces are asymmetrical.

The LWAs discussed above are based on the single-conductor SSPPs waveguide. Due to lack of a ground plane, the antennas proposed in [7]–[9] have two main beams in both the upper and lower spaces, which scan in the elevation plane. In addition, the other design with the asymmetrical modulation proposed in [8] has a single main beam scanning in the azimuth plane. The recently reported dual-layer SSPPs-transmission line (TL)-based LWAs can radiate single beam in the upper free space. Two kinds of reflector ground planes are used in [10] to reflect the back beams to the upper space. Since the reflector ground planes have a narrow band but the antenna has a wide band, the LWAs with the reflector ground planes do not always display well over the wide frequency band. A dual-conductor SSPPs-TL is used in the dual-layer LWA [11]. The dual-conductor SSPPs-TL is on the bottom layer of the LWA as the slow-wave feeding line. A series of circular patches is placed on the top layer as the radiating elements. The scanning beams are single, and the scanning region is wide, covering 66°.

In this letter, a broad scanning-angle LWA, based on the dual-conductor SSPPs-TL, is proposed. The proposed antenna is designed in a single-layer substrate. The basic traveling structure consists of a dual-grooved corrugated metal strip and a ground plane [12]. The microstrip SSPPs-TL is a slow-wave structure, which can confine waves within the interface of the metal surface and the dielectric tightly. A set of metallic posts is arranged alternately along two sides of the microstrip SSPPs-TL, which can convert SSPPs to radiation waves. The main beam of the proposed antenna is single with a wide scanning region from −30° to 51°. The structure of the proposed antenna is compact and simple to design.

Manuscript received May 17, 2018; revised June 11, 2018 and July 5, 2018; accepted July 7, 2018. Date of publication July 12, 2018; date of current version August 2, 2018. This work was supported by the National Natural Science Foundation of China under Grant 61301093. *(Corresponding author: Dujuan Wei.)*

The authors are with the School of Electrical and Information, Northwestern Polytechnical University, Xi'an 710129, China (e-mail: weidj@mail.nwpu.edu.cn; jianyingli@nwpu.edu.cn; maxwellycn@163.com; qi_yangxiao@163.com; guangweiyang@mail.nwpu.edu.cn).

Digital Object Identifier 10.1109/LAWP.2018.2855178

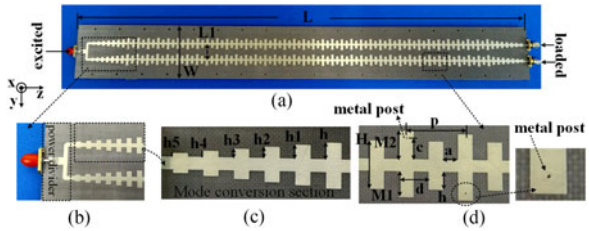

Fig. 1. Configuration of the proposed antenna. (a) Overall structure. (b) Feeding network. (c) Mode-conversion section. (d) Unit cell. $L = 556$ mm, $W = 66$ mm, $L1 = 20$ mm, $p = 12$ mm, $d = 6$ mm, $a = 3$ mm, $H = 10$ mm, $h = 3.7$ mm, $h1 = 3.2$ mm, $h2 = 2.7$ mm, $h3 = 2.2$ mm, $h4 = 1.7$ mm, $h5 = 1.2$ mm, $M1 = 5.3$ mm, $M2 = 5.8$ mm, and $c = 4.3$ mm.

II. Antenna Design and Analysis

A. Antenna Configuration

Fig. 1 illustrates the configuration of the proposed antenna, which is a periodical LWA based on the microstrip SSPPs-TL.

The proposed antenna consists of the microstrip power divider, two mode-conversion sections, and two SSPPs-TL-based antenna arrays. The mode-conversion section is a segment of the gradient microstrip SSPPs-TL, as shown in Fig. 1(c), which can effectively realize the impedance matching from the power divider to the microstrip SSPPs-TL and provide excellent wavevector conversion between them [12]. The proposed periodic LWA is formed by unit cells with metal posts and subs. It can be seen that Fig. 1(d) describes the detail of a unit cell of the proposed antenna. Along two sides of the SSPPs-TL, a set of metallic posts connects the upper and lower conductors in a staggered manner, which can convert SSPPs to radiation waves. These shorting stubs by the metallic posts are the radiation elements of the proposed LWA. The input port of the divider is excited, and matching impedances are loaded at two ends of the proposed antenna to dissipate the residual power in the terminals.

The dielectric substrate F4B is utilized in the proposed antenna (size: 556 mm × 66 mm × 1 mm, $\varepsilon_r = 2.65$). The lengths of the stub shorting by the post are $M1$ and $M2$. The diameter of the post is 0.2 mm, and the position of the post is c from the groove edge. Generally, the periodic LWA has the open stopband (OSB) effect at the broadside without any special precaution. The OSB of the proposed antenna can be suppressed by optimizing the position and diameter of the metal posts and the lengths of the stubs. The conversion section is a segment of the gradient SSPPs-TL, the depths of which are h, $h1$, $h2$, $h3$, $h4$, and $h5$. The period of the proposed antenna is p. For the SSPPs unit cell, the total height is H, the period is d, and the depth and width of the groove are h and a, respectively. The dispersion curve of the proposed antenna is mainly controlled by the depth of the groove h. The distance between two arrays is $L1$.

B. Operation Mechanism

The microstrip SSPPs-TL is used as the guiding wave line for the proposed LWA. The dispersion curves of the microstrip SSPPs-TL with various depths of the grooves ($h = 0$, 2, and 3.7 mm) are shown in Fig. 2. When $h = 0$, the SSPPs-TL becomes the microstrip line, and the dispersion curve approaches $k_0/\sqrt{\varepsilon_r}$ against the frequency. It is observed that the dispersion curve gradually deviates from the microstrip line when the groove depth increases from 0 to 3.7 mm. The guided wavelength of the SSPPs-TL becomes increasingly shorter with the increase in the groove depth h. The E-field distribution of the SSPPs-TL with $h = 3.7$ mm at 5.8 GHz in *xoz* and *yoz* planes is inserted in Fig. 2. The E-field exponentially decays in the free space, which means that the microstrip SSPPs-TL can confine the guiding waves in the structure tightly. Additionally, two SSPP unit cells have a 180° phase shift, which is in agreement with the point (0.5, 5.8 GHz) of the dispersion curve in Fig. 2.

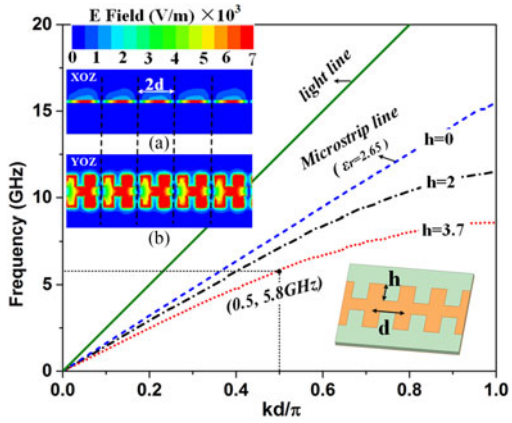

Fig. 2. Dispersion curves of the SSPPs-TL and E-field distribution with $h = 3.7$ mm at 5.8 GHz. (a) *xoz* plane. (b) *yoz* plane. $H = 10$ mm, $d = 6$ mm, and $a = 3$ mm.

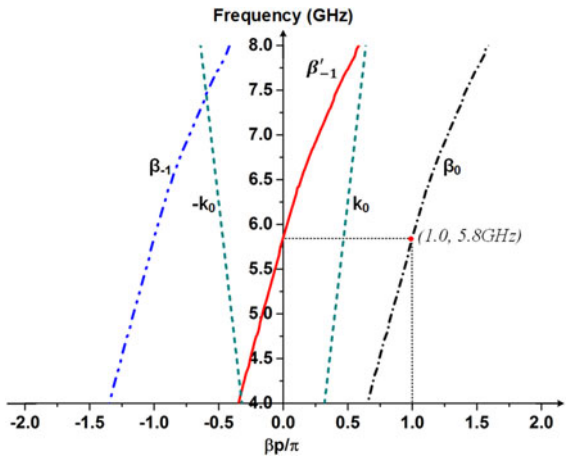

Fig. 3. Dispersion diagram from (1) and (2).

As analyzed above, waves are confined tightly in the microstrip SSPP-TL. A way of exciting the radiation waves from the slow-wave guiding structure is to introduce the discontinuous periodical unit cells. A stub with a shorting metal post is utilized in the proposed antenna as the discontinuous unit cell. When the discontinuous unit cells with period p are introduced in the SSPPs-TL, infinitely many space harmonics are generated according to Bloch–Floquet theory. The phase constant of the nth-order space harmonics of the antenna with the posts along one side is given by

$$\beta_n = \beta_0 + \frac{2\pi n}{p}, \quad n = 0, \pm 1, \pm 2, \ldots \tag{1}$$

where β_0 and β_n are the phase constants of the fundamental and nth-order space harmonics, respectively. The dispersion curves of the dominant mode and the first-order mode are illustrated in Fig. 3, which are both in the slow-wave region. The surface current of the corresponding structure is shown in Fig. 4(b).

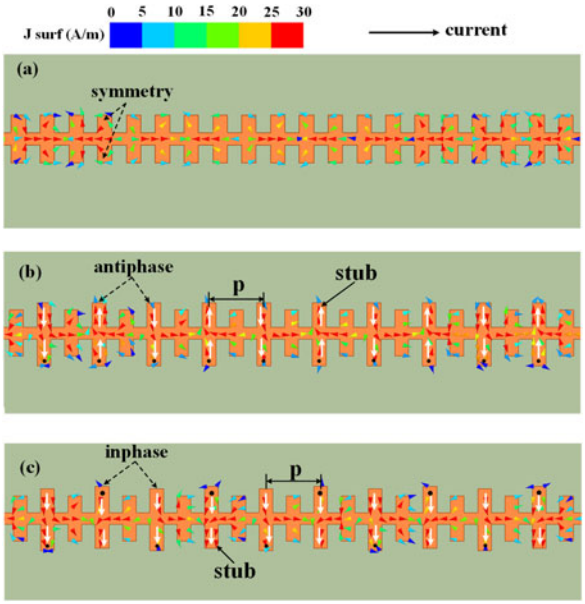

Fig. 4. Current distribution at 5.8 GHz. (a) SSPP-TL. (b) Posts along one side. (c) Posts staggered along two sides.

The currents along the adjacent stubs in Fig. 4(b) are antiphase. Therefore, the antenna with the stubs shorting by the posts along one side still cannot leak the waves out.

To obtain the leaky waves in the free space, the dispersion curve should be in the fast-wave region. It can be seen from Fig. 3 that the phase reversal should be introduced to provide an extra frequency-independent 180° phase shift per unit cell. An available way to get the phase reversal per unit cell is to stagger the metal posts along two sides of the SSPPs-TL. The expression of the space harmonics [13] is transformed from (1) into

$$\beta'_n = \beta_0 + \frac{(2n+1)\,\pi}{p}, \quad n = 0, \pm 1, \pm 2, \ldots. \tag{2}$$

When $n = -1$, the dispersion curve β'_{-1} appears in the fast-wave region in Fig. 3. The surface current of the corresponding structure is shown in Fig. 4(c), which has a 180° phase shift per unit cell, as compared with that of Fig. 4(b).

Therefore, the proposed antenna with the staggered posts along two sides of the SSPPs-TL can radiate waves at the first-order mode. The broadside frequency is 5.8 GHz, where the phase constant β'_{-1} is 0. In the frequency band below 5.8 GHz, the proposed antenna scans in the backward region. In contrast, the proposed antenna scans in the forward region.

As shown in Fig. 4(a), the structure of the SSPPs-TL is symmetrical on the *xoz* plane, so the currents on two sides of the SSPPs-TL are also symmetrical. In Fig. 4(b), a set of metallic posts with period p (two SSPPs unit cells) connects the upper and lower conductors along one side of the microstrip SSPPs-TL. The set of posts breaks the symmetry of the structure. One side of the SSPPs-TL is open, and the other side with the posts is short, which leads to the current in phase on the short and open sides. However, the current on the adjacent stubs with period p is antiphased, which is coincident with the point (1.0, 5.8 GHz) in Fig. 3. Therefore, the antenna in Fig. 4(b) cannot achieve good radiation performances. Fig. 4(c) shows that the metal posts are arranged along two sides of the microstrip SSPPs-TL in a staggered manner. As the posts are arranged alternately along two sides of the SSPPs-TL, an extra frequency-independent 180° phase shift per unit cell is introduced, which leads to the current in phase on the adjacent stubs. Therefore, the antenna in Fig. 4(c) will have good radiation properties at broadside.

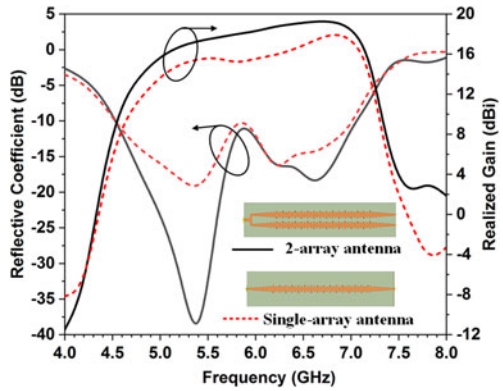

Fig. 5. Working performances of the two-array antenna and the single-array antenna.

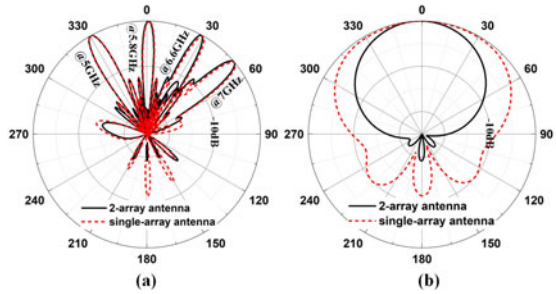

Fig. 6. Normalized radiation patterns of the two antennas. (a) H-plane from 5 to 7 GHz. (b) E-plane at 5.8 GHz.

C. Array-Antenna Performances

The working performances of the single-array antenna and the two-array antenna are compared in Figs. 5 and 6. Both antennas are loaded by matching impedances at ends. Over the working frequency band from 5 to 7 GHz, both antennas have a good impedance matching. The gain of the two-array antenna is obviously higher than that of the single-array antenna, and a 3 dBi increase is notably observed at the broadside. The beam directions of the two antennas are identical in the H-plane, and the two-array antenna has narrower beamwidth in the E-plane.

III. Simulated and Measured Results

The proposed antenna is simulated, then manufactured and measured. The reflective coefficient and the radiation efficiency of the proposed antenna are described in Fig. 7. One port is excited, and the other two ports are loaded by 50 Ω impedances. The reflection coefficient is below −10 dB from 4.5 to 7 GHz, and the measured results have a good trend with the simulated result. From 5 to 7 GHz, the radiation efficiency is more than 60%. The OSB is suppressed at broadside to a large extent, where the simulated reflective coefficient is below −10.2 dB and the realized gain in Fig. 9 has no deterioration.

Fig. 8 displays the normalized radiation patterns at 5, 5.8, 6.6, and 7 GHz, which show that the proposed antenna has good directivity and frequency-scanning property. The proposed

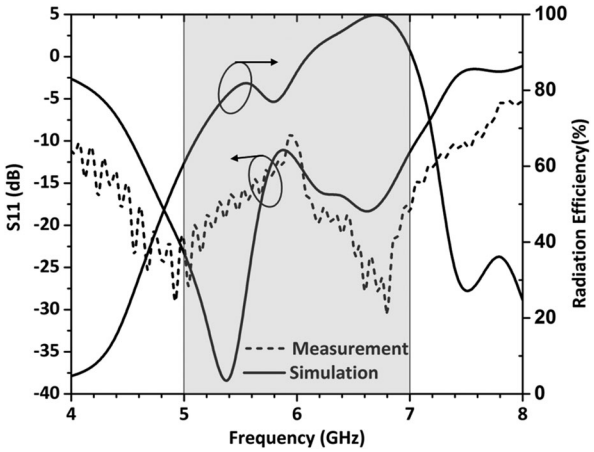

Fig. 7. Measured and simulated reflective coefficients.

TABLE I
COMPARISON OF PROPOSED ANTENNA AND PREVIOUS WORKS

Ref.	Band (GHz)	Beam	Size (mm)	Angle (deg)	Max Gain (dBi)
[7]	6-9	Dual	8.5λ	-30°-25°	8.2-11.2
[8]	8.7-9.9	Dual	11.5λ	26.1°-46.3°	12.2
[8]	8.5-9.8	Single	15.7λ	-10°- 8° (azimuth)	15.2
[9]	10.4-24.5	Dual	11.3λ	-50°-30°	9.5-12
[10]	4.5-6.5 (PEC)	Single	6.6λ	-32°-13°	14.1 (<3)
[10]	4.5-6.5 (AMC)	Single	6.6λ	-22°-21°	13.9 (> 3)
[11]	11-15	Single	5.7λ	-32°-34°	14.2 (<1.6)
Pro.	**5.0-7.0**	**Single**	**10.7λ**	**-30°-51°**	**13.8-18.1 (single array) 15.9-19.4 (two arrays)**

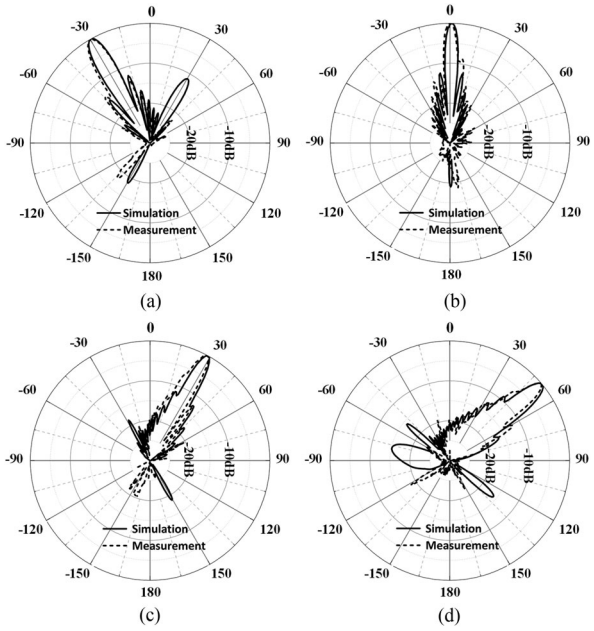

Fig. 8. Normalized radiation patterns of the proposed antenna. (a) 5 GHz. (b) 5.8 GHz. (c) 6.6 GHz. (d) 7 GHz.

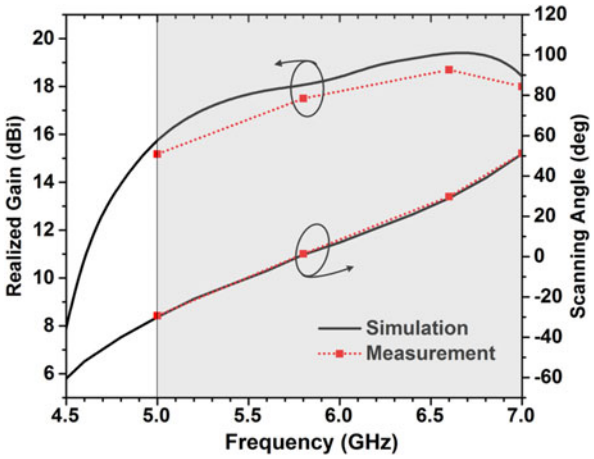

Fig. 9. Peak gain and beam-scanning angle against the frequency.

antenna with a single main beam would have a wider application field than the groundless SSPPs-TL-based LWAs with dual main beams. The proposed antenna can cover the wide scanning region from −30° at 5 GHz, from the broadside at 5.8 GHz and 29° at 6.6 GHz, to 51° at 7 GHz. The sidelobe levels (SLLs) of the scanning beam patterns from −30° to 30° are less than −11.7 dB. With the frequency increasing, the radiation patterns at the larger scanning angles have higher SLLs arriving at −9 dB. The measured results have a good agreement with the simulated patterns.

The realized gain and the beam-scanning angle of the proposed antenna are described in Fig. 9. The −10 dB impedance band is from 4.5 to 7 GHz. The realized gain decreases rapidly at the lower band because of the lower radiation efficiency. Over the frequency band from 5 to 7 GHz, the simulated realized gain is from 15.9 to 19.4 dBi. The measured gains are slightly less than the simulation gains because of dielectric attenuation, manufacture tolerance, and test tolerance. The scanning angle of the proposed antenna covers 81° from −30° to 51°. The simulated and measured angles agree.

The comparison of the proposed antenna and previous works is given in Table I. The length of the antennas in Table I are according to the broadside frequency. The proposed antenna, using a layer of dielectric substrate, is able to cover an 81° scanning range with a single beam in the *C*-band.

IV. CONCLUSION

A microstrip SSPPs-TL-based LWA with the wide scanning region is proposed in this letter. The microstrip SSPPs-TL is a planar dual-conductor SSPPs-TL, which consists of a two-edged grooved corrugated strip and a ground plane. As the SSPPs-TL confines the waves in the structure tightly, a set of metallic posts shorting the corrugated strip to the ground plane in a staggered manner is introduced to convert SSPPs to radiation waves. By increasing the depth of the groove, the group velocity of the waves decreases, which leads to a wide scanning region.

The proposed antenna has good radiation performances. Over the working frequency band from 5 to 7 GHz, the frequency-scanning beam covers a wide region in the upper free space from −30° to 51°, and the realized gain is increased from 15.9 to 19.4 dBi. A prototype is fabricated and measured, which confirms the design theory and the simulation results.

REFERENCES

[1] R. C. Johnson and H. Jasik. *Antenna Engineering Handbook*. New York, NY, USA: McGraw-Hill, 1993.

[2] H. Raether, "Surface Plasmons on smooth and rough surfaces and on gratings," in *Springer Tracts in Modern Physics*. New York, NY, USA: Springer-Verlag, 1988, pp. 4–39.

[3] J. B. Pendry, L. Martín-Moreno, and F. J. Garcia-Vidal, "Mimicking surface plasmons with structured surfaces," *Science*, vol. 305, pp. 847–848, Aug. 2004.

[4] F. J. Garciavidal, L. Martín-Moreno, and J. B. Pendry, "Surfaces with holes in them: New plasmonic metamaterials," *J. Opt. A, Pure Appl. Opt.*, vol. 7, no. 2, pp. S97–S101, 2005.

[5] H. F. Ma, X. P. Shen, Q. Cheng, W. X. Jiang, and T. J. Cui, "Broadband and high-efficiency conversion from guided waves to spoof surface plasmon polaritons," *Laser Photon. Rev*, vol. 8, no. 1, pp. 146–151, 2014.

[6] T. J. Cui and X. P. Shen, "Spoof surface plasmons on ultrathin corrugated metal structures in microwave and terahertz frequencies." in *Proc. IEEE 7th Int. Congr. Adv. Electromagn. Mater. Microw. Opt.*, 2013, pp. 537–539.

[7] J. Y. Yin *et al.*, "Frequency-controlled broad-angle beam scanning of patch array fed by spoof surface plasmon polaritons," *IEEE Trans. Antennas Propag.*, vol. 64, no. 12, pp. 5181–5189, Dec. 2016.

[8] S. K. Gu, H. F. Ma, B. G. Cai, and T. J. Cui, "Continuous leaky-wave scanning using periodically modulated spoof plasmonic waveguide," *Sci. Rep.*, vol. 6, 2016, Art. no. 29600.

[9] A. Kianinejad, Z. N. Chen, and C. W. Qiu, "A single-layered spoof-plasmon-mode leaky wave antenna with consistent gain," *IEEE Trans. Antennas Propag.*, vol. 65, no. 2, pp. 681–687, Feb. 2017.

[10] Q. L. Zhang, Q. F. Zhang, and Y. F. Chen, "Spoof surface plasmon polariton leaky-wave antennas using periodically loaded patches above PEC and AMC ground Planes," *IEEE Antennas Wireless Propag. Lett.*, vol. 16, pp. 3014–3017, 2017.

[11] D. F. Guan, P. You, Q. F. Zhang, Z. H. Lu, S. W. Yong, and K. Xiao, "A wide angle and circularly polarized beam scanning antenna based on microstrip spoof surface plasmon polariton transmission line," *IEEE Antennas Wireless Propag. Lett.*, vol. 16, pp. 2538–2541, 2017.

[12] W. J. Zhang, G. Q. Zhu, L. G. Sun, and F. J. Lin, "Trapping of surface plasmon wave through gradient corrugated strip with underlayer ground and manipulating its propagation," *Appl. Phys. Lett.*, vol. 106, no. 2, Jan. 2015. Art. no. 021104.

[13] N. Yang, C. Caloz, and K. Wu, "Full-space scanning periodic phase-reversal leaky-wave antenna," *IEEE Trans. Microw. Theory Techn.*, vol. 58, no. 10, pp. 2619–2632, Oct. 2010.